Verfahrenstechnik auf einem neuen Level? It takes #HumanChemistry

Wir suchen kreative Ingenieurinnen und Ingenieure, die mit uns gemeinsam neue Wege gehen wollen – mit Fachwissen, Unternehmertum und Kreativität für innovative Lösungen. Informieren Sie sich unter:

evonik.de/karriere

EVONIK
Leading Beyond Chemistry

Received: 22 March 2021 | Revised: 10 July 2021 | Accepted: 1 September 2021

DOI: 10.1002/bit.27937

ARTICLE

BIOTECHNOLOGY AND BIOENGINEERING WILEY

A high cell density perfusion process for Modified Vaccinia virus Ankara production: Process integration with inline DNA digestion and cost analysis

Gwendal Gränicher[1] | Masoud Babakhani[1,2] | Sven Göbel[1,3] | Ingo Jordan[4] | Pavel Marichal-Gallardo[1] | Yvonne Genzel[1] | Udo Reichl[1,2]

[1]Bioprocess Engineering Group, Max Planck Institute for Dynamics of Complex Technical Systems, Magdeburg, Germany

[2]Chair for Bioprocess Engineering, Faculty of Process- and Systems Engineering, Otto-von-Guericke-University Magdeburg, Magdeburg, Germany

[3]Institute of Biochemical Engineering, Faculty 4 - Energy-, Process- and Bio-Engineering, University of Stuttgart, Stuttgart, Germany

[4]ProBioGen AG, Berlin, Germany

Correspondence
Yvonne Genzel, Bioprocess Engineering Group, Max Planck Institute for Dynamics of Complex Technical Systems, Sandtorstr. 1, 39106 Magdeburg, Germany.
Email: genzel@mpi-magdeburg.mpg.de

Present address
Gwendal Gränicher, AAV Technical Operations, DiNAQOR, Wagistrasse 25, Schlieren, Zurich 8952, Switzerland.

Abstract

By integrating continuous cell cultures with continuous purification methods, process yields and product quality attributes have been improved over the last 10 years for recombinant protein production. However, for the production of viral vectors such as Modified Vaccinia virus Ankara (MVA), no such studies have been reported although there is an increasing need to meet the requirements for a rising number of clinical trials against infectious or neoplastic diseases. Here, we present for the first time a scalable suspension cell (AGE1.CR.pIX cells) culture-based perfusion process in bioreactors integrating continuous virus harvesting through an acoustic settler with semi-continuous chromatographic purification. This allowed obtaining purified MVA particles with a space-time yield more than 600% higher for the integrated perfusion process (1.05×10^{11} $TCID_{50}/L_{bioreactor}$/day) compared to the integrated batch process. Without further optimization, purification by membrane-based steric exclusion chromatography resulted in an overall product recovery of 50.5%. To decrease the level of host cell DNA before chromatography, a novel inline continuous DNA digestion step was integrated into the process train. A detailed cost analysis comparing integrated production in batch versus production in perfusion mode showed that the cost per dose for MVA was reduced by nearly one-third using this intensified small-scale process.

KEYWORDS
semi-continuous production, steric exclusion chromatography, suspension cell culture in bioreactor, upstream and downstream processing, viral vector

1 | INTRODUCTION

To date, the implementation of an integrated perfusion process is an option to decrease manufacturing costs and to potentially increase the quality of a product (Bielser et al., 2018; Walther et al., 2015, 2019; Xu & Chen, 2016). A considerable amount of research has been conducted on the integrated continuous production of recombinant proteins such as monoclonal antibodies (Godawat et al., 2015; Karst et al., 2017, 2018; Konstantinov & Cooney, 2015; Pinto et al., 2019; Warikoo et al., 2012). However, to our knowledge, options for an integrated viral

vector production in perfusion mode have not been reported in the literature, although it seems evident that this could offer improvements in biopharmaceutical product quality (Allison et al., 2015).

Similar to recombinant protein manufacturing, process intensification for viral vectors could be a solution to lower production costs and space requirements for culture vessels. Process intensification may also help to satisfy the increasing demand for viral vectors at high concentrations for R&D, clinical trials, and commercialization (Kaemmerer, 2018; van der Loo & Wright, 2015). Intensification can be achieved with bioreactors coupled to devices for harvesting of infectious units with subsequent continuous purification. A techno-economic analysis could provide insights about cost differences between a batch and a perfusion process for viral vector production (Cameau et al., 2019; Gränicher et al., 2020; Pearson, 2020), similarly to recombinant protein production (Klutz et al., 2016; Lim et al., 2006; Pleitt et al., 2019; Pollock et al., 2013). This could allow identifying key factors and bottlenecks allowing cost-savings. To our knowledge, only a few studies in bioprocess economics related to viral vector manufacturing for gene therapy have been performed, so far (Cameau et al., 2019; Comisel et al., 2020). Up to now, no studies have evaluated the costs of virus production using a perfusion system linked to a suspension cell culture.

The establishment of integrated perfusion systems requires the use of cell retention systems that allow high process robustness, scalability, and continuous virus harvesting. In addition to cell retention as a preemptive processing step, continuous virus harvesting could also result in higher production yields and better product quality (Gränicher et al., 2020; Manceur et al., 2017; Petiot et al., 2011).

To date, membrane-based alternating tangential flow (ATF) modules are mainly used for the production of biopharmaceuticals in perfusion mode (Bielser et al., 2018). Surprisingly, however, product retention has been observed even with membranes that have pore sizes exceeding significantly the virus diameter (Genzel et al., 2014; Gränicher et al., 2020; Nikolay et al., 2018). Most likely, virus particle retention is due to filter fouling and cake formation associated with increasing cell lysis at the late infection stages. This concerns in particular the accumulation of host cell DNA and cell debris in the 100 nm range (Wang et al., 2017). Similar effects have been observed for recombinant protein production in perfusion mode but could be avoided by using membranes with pore sizes more than or equal to 1 µm (Pinto et al., 2019; Wang et al., 2019).

The acoustic settler technology is an alternative to ATF for continuous virus harvesting and can be scaled to a perfusion flow rate of 1000 L/day (Gränicher et al., 2020, 2020; Manceur et al., 2017). Such a device circumvents the pore size limitations of ATF modules, but temperature elevation in the acoustic flow chamber needs to be controlled to maintain virus stability. This can be achieved mainly through the adjustment of the perfusion flow rate during operation (Gränicher et al., 2020).

The use of an online probe measuring the electric capacitance allows to monitor cell concentration, cell size, metabolic state, apoptosis, and viral infection (Justice et al., 2011; Nikolay et al., 2018; Petiot et al., 2017; Vazquez-Ramirez et al., 2019). In addition, it was shown that capacitance sensors can be used to determine other key process parameters, that is, the optimal time of virus harvesting (Grein et al., 2018; Negrete et al., 2007).

Here, we present for the first time a fully integrated cell culture-based perfusion process allowing an end-to-end viral vector production at high cell densities. The avian suspension cell line AGE1.CR.pIX was used to produce Modified Vaccinia virus Ankara (MVA), which is a promising vector for vaccination against various infectious diseases and certain forms of cancers (https://ClinicalTrials.gov). An acoustic filter was utilized for continuous harvesting of MVA. In addition, a capacitance sensor was used to monitor cell growth, control the perfusion rate, and decide on the time of virus harvesting. For viral vector purification, a semi-continuous method using membrane-based steric exclusion chromatography (SXC) was directly linked to the continuous virus harvest stream. Achieving a maximum viable cell concentration (VCC) of up to 37×10^6 cells/mL during virus production (dilution step at 12 hpi), the space-time yield (STY) of purified MVA particles for the process established was 1.05×10^{11} TCID50/$L_{bioreactor}$/day. The production setup allowed an overall recovery of virus particles of 50.5%, with a concentration of host cell DNA per dose below the limits typically set for human vaccines by regulatory authorities. Furthermore, we could reduce significantly the host cell DNA level by integrating a DNA digestion step in continuous mode before chromatography. The collected data allowed then for an academic techno-economic analysis between batch and perfusion.

2 | MATERIALS AND METHODS

2.1 | Cells, virus, and media

An immortalized Muscovy duck retina suspension AGE1.CR.pIX cell line was used as a host for production of MVA-CR19.GFP (infectious titer: 4.1×10^8 $TCID_{50}$/ml), which contains a green-fluorescent-protein insertion cassette (Jordan et al., 2020). Chemically-defined CD-U5 medium (Biochrom-Merck) supplemented with 2 mM L-glutamine (Sigma-Aldrich) and 10 ng/ml recombinant insulin-like growth factor (LONG-R^3 IGF, 91590C; Sigma-Aldrich) was used for cell growth. Shake flasks were used for cells maintenance and for inoculation of the bioreactors as described earlier (Gränicher et al., 2020; Jordan et al., 2011).

2.2 | Bioreactor cultivation

To compare MVA production in batch or in perfusion mode, the cells were cultivated in bioreactors in batch or in perfusion mode.

2.2.1 | Batch cultivations

DASGIP bioreactors (1 L maximum working volume; Eppendorf AG) were inoculated at a VCC of 1.0×10^6 cells/ml (initial working volume

(V_w) = 500 ml). A stirring speed of 145 rpm using a pitched-blade impeller was chosen. The pH was maintained at 7.2 through CO_2 sparging and NaOH (0.55 M) base addition. The dissolved oxygen level (DO) was maintained at 40% air saturation using a drilled-hole L-sparger. Temperature was maintained at 37°C. Once the VCC reached 4×10^6 cells/ml, the V_w was doubled from 500 ml to 1000 ml by addition of fresh medium and cells were infected at a multiplicity of infection (MOI) of 0.05 infectious units/cells ($TCID_{50}$ assay). Seed virus (MVA-CR19.GFP; Section 2.1) was treated for 1 min in a sonication water bath at 45 kHz before usage. Virus production in batch mode was done according to the optimized method described by Lohr (2014). The integrated virus production in batch mode was performed in triplicate with three parallelized bioreactors using the same cell culture seed train.

2.2.2 | Perfusion cultivation

A Biostat bioreactor (1 L maximum V_w; Sartorius AG) was used to cultivate the cells. DO was set to 40% using a drilled-hole L-sparger, using pure oxygen. The pH was kept to 7.2 using CO_2 and temperature was controlled at 37°C. The system was agitated using a pitched-blade impeller at 180 rpm. The perfusion bioreactor was inoculated at a VCC of 1×10^6 cells/ml (V_w = 550 ml) and perfusion was started at a VCC of 6×10^6 cells/ml. The same medium used in batch cultures was used for the perfusion processes (Section 2.2-1).

An acoustic settler device with a power of 2 W and a frequency of 2.1 MHz was used for cell retention. The parameters of the acoustic settler were set as reported in a previous publication (Gränicher et al., 2020). A constant recirculation flow rate of five reactor volumes per day (day^{-1}) was applied for the acoustic settler system. Before infection, a cell-specific perfusion rate (CSPR) of 50 pL/cell/day was chosen. For run 1 only, an online capacitance probe and a Watson–Marlow harvest pump connected to a controller (ArcView Controller 265) were used to maintain the CSPR at a steady state during the cell growth phase (Nikolay et al., 2020). The sensor was operating in a frequency range of 1–10 MHz and the signal was recorded every 12 min. The correlation between the VCC and the permittivity signal was determined by linear regression (the resulting slope corresponds to the "cell factor"). For run 2, the CSPR was adjusted manually by adjusting the pump once a day based on off-line VCC measurements.

The bioreactor cell culture medium was replaced using a perfusion rate of 8–12 day^{-1} for 2–3 h before infection. The cells were then infected at a VCC of 50×10^6 cells/ml with MVA-CR19.GFP at an MOI of 0.05 infectious units/cell ($TCID_{50}$ assay), as described in Section 2.2. The perfusion was halted and the V_w was increased from 550 ml to 1000 ml between 0 and 12 h postinfection (hpi) similar to the process described by Vazquez-Ramirez et al. (2019). For the perfusion run 1, the V_w was increased continuously between 2 and 12 hpi. For the perfusion run 2, the V_w was increased continuously between 11 and 12 hpi. Afterward, a constant perfusion rate of 1.75 day^{-1} was maintained. To reduce medium consumption for this experiment, the V_w was reduced from 1000 ml to 800 ml at 36 hpi. Accordingly, the harvest pump flow rate had to be decreased from 66.7 ml/h to 54 ml/h to maintain the perfusion rate at a steady state for subsequent purification processes. Virus release in the cell culture supernatant was monitored using the permittivity signal $\Delta\varepsilon_{max}$, in pF/cm. The cell membrane capacitance (C_m, µF/cm^2) and intracellular conductivity (σ_i, mS/cm) were calculated as described previously (Petiot et al., 2017). With the onset of virus release (about 40 hpi), the harvesting line was directed to a harvest bottle (bottle B1 in Figure 1) kept at 4°C, and later purified. Harvesting of MVA particles released was initiated 10.6 h after the maximum permittivity signal was reached. This corresponded to the time when about 8%–10% of the total number of infectious virions (Vir_{tot}, bioreactor, and harvest vessel, Section 2.4) was released from the infected cells (see Section 3.3). This definition was chosen to ensure high titers in the harvesting line (>10^8 $TCID_{50}$/ml) and to avoid any product concentration step before chromatography. Samples during cell culture were taken every 8–14 h.

2.3 | Process integration

To match the scenarios for integrated virus production, both batch and perfusion cultivations were performed in bioreactors (Section 2.2). MVA bioreactor harvests were purified as described below except for perfusion run 2. In the case of the perfusion strategy, MVA particles were continuously harvested and semi-continuously purified as illustrated in Figure 1. A photo of the experimental setup is shown in the Appendices (Figure A1).

Due to the lytic nature of MVA replication, the upstream process was not fully continuous but split into two phases: a cell growth phase, in which cells were cultivated from 1×10^6 cells/ml to 50×10^6 cells/ml, and a virus production phase, initiated when cells were infected with MVA and continued with a dilution step at 12 hpi (inducing host cell death visible from 75 hpi onwards) (Tapia et al., 2016). The continuously harvested virus raw material was semi-continuously purified. Therefore, virus particles that passed the cell retention device were continuously filtered and treated with endonuclease before purification by SXC in bind-elute mode using an ÄKTA Pure system (Figure 1).

2.3.1 | Harvest and clarification

Batch

Once the viability of the infected culture dropped to 70%, harvesting was initiated and 95.3% of the V_w was first clarified using the acoustic settler (10 L acoustic chamber version; SonoSep Technologies) with an acoustic power of 3 W and a frequency of 2.1 MHz, at a flow rate of 252 ml/h. Sodium azide 0.05% v/v was added to the harvest to reduce contamination risk. Then 700 mM salt (NaCl, NaBr, and KCl) was added and the supernatant was depth filtered using a polypropylene filter (PP3 Sartopure, 0.45 µm pore size, 120 cm^2

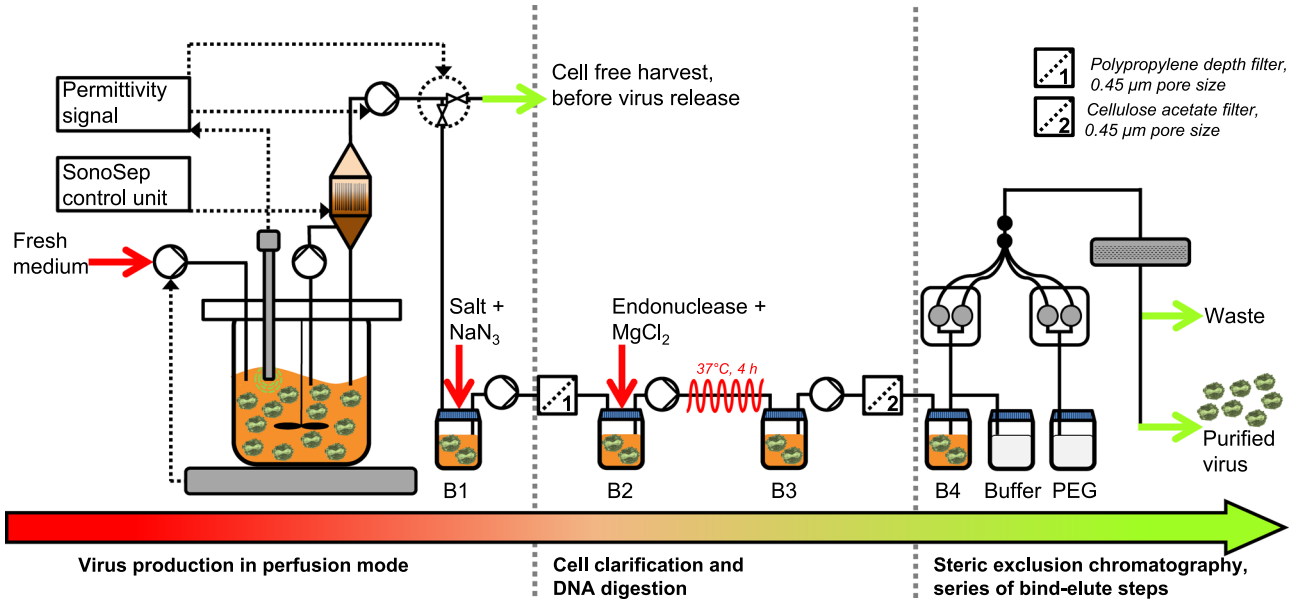

FIGURE 1 Scheme of an integrated process for cell culture-based virus production in perfusion mode. The integrated Modified Vaccinia virus Ankara (MVA) production is separated into three main steps, separated by gray vertical dotted lines: (1) Virus production in perfusion mode using an acoustic filter, (2) cell clarification and DNA digestion, and (3) steric exclusion chromatography (SXC) as a series of bind-elute steps. MVA is produced using AGE1.CR.pIX cells grown in suspension in a stirred tank bioreactor. To achieve high cell concentrations, the cells are retained in the bioreactor while the cell-free medium is continuously harvested through the acoustic chamber controlled by the SonoSep control unit (acoustic filter as perfusion system). To allow a constant bioreactor working volume and weight, a fresh medium is added into the bioreactor through a peristaltic pump controlled by a scale. During the cell growth phase, the harvest flow rate is controlled based on the estimation of the viable cell concentration using a capacitance sensor. After infection, a decrease in the permittivity signal indicates virus particle release and initiates cell clarification and subsequent chromatography steps. The harvest containing MVA (which was the first cell clarified through the acoustic settler) is collected into bottle B1. Salt and sodium azide (NaN_3) are added to bottle B1 as well. The virus harvest is then continuously filtered through a polypropylene depth filter with 0.45 µm pore size (Filter 1). For continuous endonuclease digestion (addition of endonuclease and magnesium chloride ($MgCl_2$) in bottle B2), the harvest is incubated into a plug-flow reactor (indicated with the coiled red tube) at 37°C with a residence time of 4 h. The endonuclease-digested product is continuously collected into bottle B3. After another filtration step using cellulose acetate depth filter with 0.45 µm pore size (Filter 2), the harvest is collected into bottle B4 at 4°C. An ÄKTA Pure 25 system is used to purify the virus harvest using membrane-based SXC operated in a semi-continuous bind-elute mode; the composition of buffer solutions (including buffer solution with PEG) used in purification are described in Section 2.3-3. Finally, purified MVA is collected into 50 ml tubes (not illustrated). The color of the horizontal arrow going from red to green illustrates the stepwise purification of the MVA and the removal of contaminating host cell DNA

(5051306P4--OO--B) or 4.5 cm^2 (5055306PV--LX--C) filtration surface; Sartorius AG), at a constant flow rate of 0.45 ml/min/cm^2 and a filtration capacity of at least 126 L/m^2. The clarified cell culture supernatant was subsequently treated with endonuclease and further clarified as described in Section 2.3-2.

Perfusion

As described in Section 2.2-2, the bioreactor was continuously harvested at 40 hpi onwards. The cell culture harvest from the acoustic settler was not suitable for direct purification using SXC as the contamination level of cells and cell debris passing through the cell retention device was too high. Therefore, the cell culture harvest was first collected in bottle B1, and salts were continuously added to reach 700 mM of NaCl, NaBr, and KCl mixture, (as illustrated in Figure 1) to avoid virus interaction with the depth filter, to stabilize virus particles and to facilitate endonuclease treatment (Table 1). Sodium azide was also continuously added to bottle B1 (Table 1). The harvest was then clarified using a polypropylene depth filter with a pore size of 0.45 µm (filtration capacity of 240 L/m^2; Sartopure PP3, 120 cm^2 filtration area), transferred to bottle B2 (Figure 1) for DNA digestion and microfiltration as described in Section 2.3-2.

2.3.2 | DNA digestion and microfiltration

Batch

DNA in the supernatant was digested using endonuclease at a final activity of 35 U/ml (DENARASE®, enzyme activity > 250 U/µl determined by the manufacturer, 20804-100k; c-Lecta), mixed with 3 mM $MgCl_2$. The cell culture supernatant was incubated in a glass bottle for 4 h at 37°C and stirred at 100 rpm using a magnetic agitator. The endonuclease step was optimized by decreasing the amount of endonuclease needed to achieve DNA depletion up to 1000-fold within 4 h. In a scouting experiment, the stability of infectious virions at 37°C was demonstrated for a period of at least 12 h (Gränicher et al., 2020). Finally, the treated cell culture

TABLE 1 Process parameters used for continuous clarification and DNA digestion of bioreactor harvests after the acoustic settler

Parameter	Cell culture harvest	NaCl, NaBr, and KCl	NaN_3	DENARASE®, diluted in PBS + 5% sucrose	$MgCl_2$
Initial concentration	–	6000 mM	6.2% v/v	1628 U/ml	176 mM
Final concentration	–	700 mM	0.08% v/v	37 U/ml	4 mM
Point of addition[a]	B1	B1	B1	B2	B2
Flow $rate_{in}$ [ml/h]	54.0	7.5	0.8	1.5	1.5
Flow $rate_{out}$ [ml/h]	62.3	62.3	62.3	65.3	65.3

Abbreviation: PBS, phosphate-buffered saline.

[a]Bottle names according to the scheme shown in Figure 1.

supernatant was filtered using 0.45 µm cellulose acetate filters (Minisart NML Syringe Filter, 6.2 cm^2 total filtration area, 16555-K; Sartorius AG) at a flow rate of 8 ml/min/cm^2 and a filtration capacity of 175 L/m^2. The treated cell culture supernatant was either stored at −80°C or directly purified through SXC, as described in Section 2.3-3.

Perfusion

The clarified cell culture broth was continuously treated in bottle B2 with 37 U/ml endonuclease (DENARASE®) and with 4 mM $MgCl_2$ (Table 1; a higher endonuclease activity and $MgCl_2$ concentration were chosen for the perfusion process compared with the batch process to ensure DNA digestion without mixing). After bottle B2, the material was continuously transferred to a coiled silicone tube (3.2 mm inner diameter, 32.5 m length, GESSULTRA-C-125-2H; VWR) with a retention time of 4 h at 37°C in an incubator. The product was collected continuously into bottle B3. The harvest from bottle B3 was filtered using 0.45 µm cellulose acetate filters (filtration capacity of 290 L/m^2; Minisart NML Syringe Filter, 6 × 6.2 cm^2 total filtration area). The filtered product was then collected in bottle B4 and stored at 4°C before the chromatography step (described in Section 2.3-3). As the process was operated continuously, the V_w of bottles B1, B2, B3, and B4 were kept constant at 180, 120, 60, and 120 ml, respectively.

2.3.3 | Purification through steric exclusion chromatography

Membrane-based SXC was performed using an ÄKTA Pure 25 system (Cytiva) as described previously (Marichal-Gallardo et al., 2017), using PBS with NaCl, NaBr, and KCl (700 mM final salt concentration) as elution buffer and polyethylene glycol (PEG, 81260-1KG; MW 6000, dissolved in PBS + 700 mM NaCl, NaBr and KCl; Sigma-Aldrich) as equilibration buffer. A total surface of 70 cm^2 of regenerated cellulose (14 × 25 mm stacked membranes, 1 µm pore size, 10410014; GE, now Cytiva) was used. Optimized purification settings (Appendices) were determined as follows: PEG concentration = 7.2% w/v, flow rate = 8.2 ml/min.

UV was monitored at a wavelength of 280 nm and 360 nm. The column was operated at 27% to 75% breakthrough of the dynamic binding capacity of the column. This allowed purifying a 45 ml sample per cycle, lasting 40 min in total, including column regeneration time. The column (XX3002500; EMD Millipore) was regenerated each time by flushing 25 ml of 2 M NaCl in 1 M NaOH. The membranes of the column were replaced every four cycles. Consecutive series of bind-elute steps allowed the purification of 67.5 ml/h of cell culture supernatant. The SXC protocol used for purification was identical for both batch and perfusion cultures.

2.4 | Analytics and yield calculations

The VCC and percentage cell viability were determined using a Vi-CELL XR (Beckman-Coulter). Glucose, glutamine, lactate, and ammonium concentrations were measured using a Bioprofile 100 plus (Nova biomedical).

For titration of the MVA-CR19.GFP strain in the supernatant, a median tissue culture infectious doses ($TCID_{50}$) assay with serial two-fold dilutions instead of 10-fold dilutions (as described by Nikolay et al. 2020) were performed, resulting in a standard deviation of ± 0.077 $log_{10}(TCID_{50}$/ml) (standard deviation of a sample measured by three operators, performed for each in triplicate). Samples purified by SXC were sonicated with a VialTweeter (UP200St, Power = 160 W, Amplitude = 100%, Pulse = 30%; Hielscher Ultrasound Technology) to dissolve virus aggregates before measurements. The total number of infectious virions measured in the harvest vessel and in the bioreactor (Vir_{tot}, based on $TCID_{50}$), the concentration of infectious virions produced ($C_{vir,\ tot}$, $TCID_{50}$/ml), the volumetric virus productivity (P_v, $TCID_{50}$/L/day), and the cell-specific infectious virus yield (CSVY, $TCID_{50}$/cell) were calculated as described previously by Gränicher et al. (2020). The STY of purified MVA was calculated based on the bioreactor V_w ($TCID_{50}/L_{bioreactor}$/day; similar calculation compared with P_v, but replacing the spent cell culture medium volume with V_w). On a linear scale, the $TCID_{50}$ assay contributes an error of +19.4/−16.3% to $C_{vir,\ tot}$, Vir_{tot}, CSVY, P_v, and STY. For perfusion, the recovery (in %) of each filtration or DNA digestion step was calculated as the ratio of the average titer after and before the step as shown in Table 2.

TABLE 2 Parameters used to calculate the recovery of each filtration or DNA digestion step in perfusion mode.

Recovery [%][a]	Average infectious virus titer between t_{n-1} and t_n before the step	Average infectious virus titer between t_{n-1} and t_n after the step
Acoustic settler filtration[b]	Bioreactor supernatant	Bottle B1[c]
Depth filtration	Bottle B1[c]	Bottle B2[c]
DNA digestion	Bottle B2[c]	Bottle B3[c]
Final filtration	Bottle B3[c]	Bottle B4[c]

[a]The recovery is calculated as the ratio of the average titer after and before the step.

[b]Ratio for the settler filtration recovery calculated similarly to the sieving coefficient calculated for recombinant protein perfusion cultures (Wang et al., 2017).

[c]Bottle names according to the scheme shown in Figure 1.

For batch cultures, the recovery was calculated stepwise as the ratio between the total number of infectious virions after and before the filtration or DNA digestion step. The average was calculated as the average recovery of three integrated batch bioreactor runs.

Recovery of SXC (in %) was calculated for each purification cycle as described earlier (Marichal-Gallardo et al., 2017). The average SXC recovery of perfusion was the mean of all cycles performed for one integrated process. To reduce the consumption of spin tubes, buffers, and regenerated cellulose, the SXC was operated 23% of the period during the virus production phase, always with 3–4 consecutive cycles (intervals <9 h). The average SXC recovery for the batch process was calculated based on the 4 × 3 purification cycles (the SXC column is replaced after four purification cycles) performed for each triplicate. The concentration of host cell DNA was measured through a qPCR assay (Rotor-Gene Q real-time PCR cycler; Qiagen), correlated with a standard host cell DNA concentration of lysed AGE1.CR.pIX cells were measured through a Picogreen assay as described earlier (Marichal-Gallardo et al., 2017). The total protein concentration was measured with a Bradford assay (Marichal-Gallardo et al., 2017). The host cell DNA and total protein per dose were calculated as described previously (Gränicher et al., 2020). One dose was considered here as equal to 10^8 plaque-forming units (PFU) (Wyatt et al., 2004), which is equivalent to 1.43×10^8 $TCID_{50}$ (ATCC, 2012).

2.5 | Economic analysis

To estimate the impact on cost per dose for an end-to-end MVA production of a batch and a perfusion system, the process simulation software SuperPro Designer v10 (Intelligen Inc.) was used. All data of upstream processing (USP) and downstream processing (DSP) relate to the cost of goods collected at the Department of Bioprocess Engineering (Max Planck Institute) for 1 L bioreactor scale in an academic environment. Using the software SuperPro Designer v10 and the data obtained at the 1 L bioreactor scale, the cost per dose for an end-to-end MVA production was estimated for the 10–1000 L bioreactor scale range. Key assumptions used to compare batch and perfusion processes: (i) Production runs over 47 weeks per year and the seed train process 65% of the time (31 weeks per year). (ii) Fill & finish costs and duration are considered the same for batch and perfusion. (iii) MVA preparations of both processes are assumed to have the same product quality. (iv) All bioreactors are assumed to operate at maximum volume capacity. (v) Indirect costs relevant for the cost of goods evaluation such as waste disposal (similarly to other cost analysis publications for viral vector production (Comisel et al., 2020)) and depreciation maintenance and plant depreciation were not considered for both systems. (vi) Costs related to QA/QC, operation of the facility, and labor was taken from default values given by the software.

3 | RESULTS

3.1 | Intensified cell culture for MVA production

First, to establish a robust process that allows for continuous harvesting and high MVA yields, two perfusion experiments using the acoustic settler (runs 1–2) were performed as described in Section 2.2-2. As a control, a batch process was operated in triplicate (runs a–c). Achieving maximal VCCs of $36.9–38.0 \times 10^6$ cells/ml during virus production (Figure 2a) (dilution at 12 hpi), an average recovery of 107 ± 18% was observed for the virus material collected after the settler (volume = 2.8–2.9 L; Figure 2b). The Vir_{tot} produced in the harvest and in the bioreactor vessel was 20.4×10^{11} and 9.1×10^{11} $TCID_{50}$ for runs 1 and 2, respectively (Figure 2b). For the batch runs, an average Vir_{tot} of $2.4 \pm 0.6 \times 10^{11}$ $TCID_{50}$ was measured. For the perfusion runs, the CSVY was 24.0 and 55.4 $TCID_{50}$/cell, and the P_v 1.43 and 2.53×10^{10} $TCID_{50}$/L/day for runs 1 and 2, respectively. As a comparison, an average CSVY of 46.9 ± 13.2 $TCID_{50}$/cell and an average P_v of $3.82 \pm 0.93 \times 10^{10}$ $TCID_{50}$/L/day were obtained for the triplicate batch runs (a)–(c) (Figure 2c,d).

3.2 | Process integration for viral vectors production

Compared to the batch processes (a)–(c), similar recovery yields and impurity levels were obtained during purification (Figure 3; DSP as in Section 2.3). Total recovery for batch (runs a–c) and perfusion

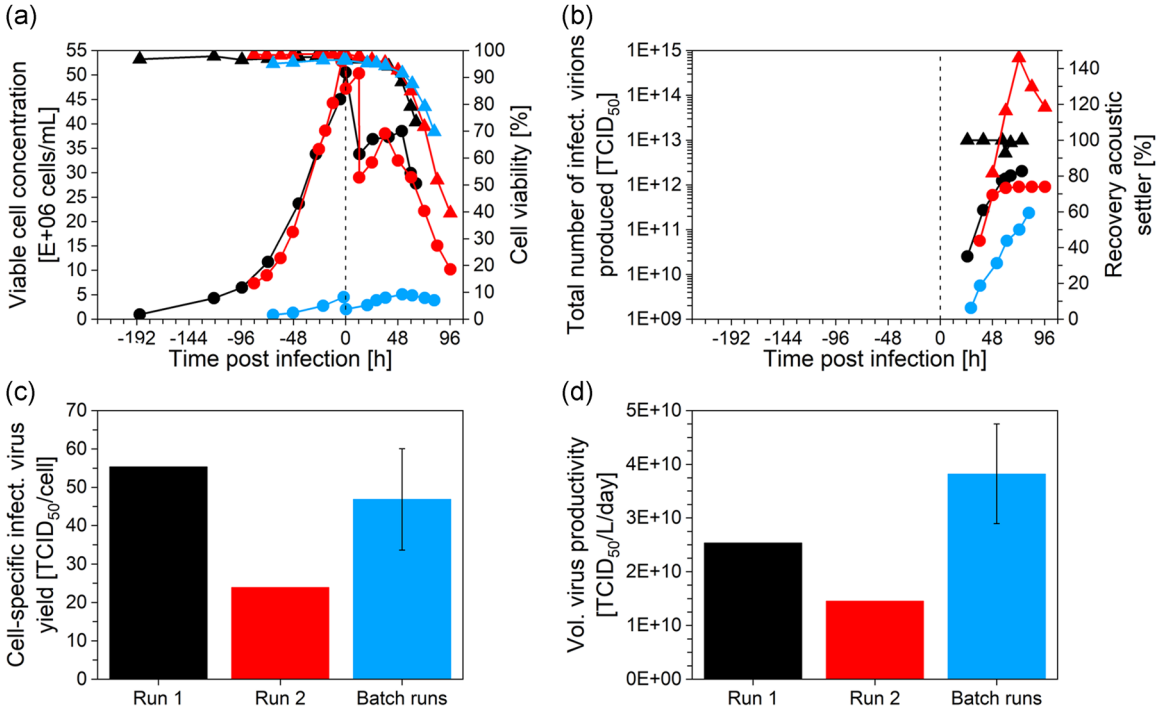

FIGURE 2 Modified Vaccinia virus Ankara (MVA) production in AGE1.CR.pIX cells in perfusion and in batch mode (stirred tank bioreactor, CD-U5 medium). (a) Viable cell concentration (●) and cell viability (▲), (b) total number of infectious virions produced (●) and recovery coefficient (from the acoustic settler filtration step) (▲), (c) cell-specific infectious virus yield, and (d) volumetric virus productivity (for infectious virions). The black, red, and blue colors correspond to run 1, run 2 (one replicate) and the batch runs (average from runs a–c, in triplicate), respectively. The error bars on graphs (c) and (d) correspond to the standard deviation of the batch runs performed in triplicate

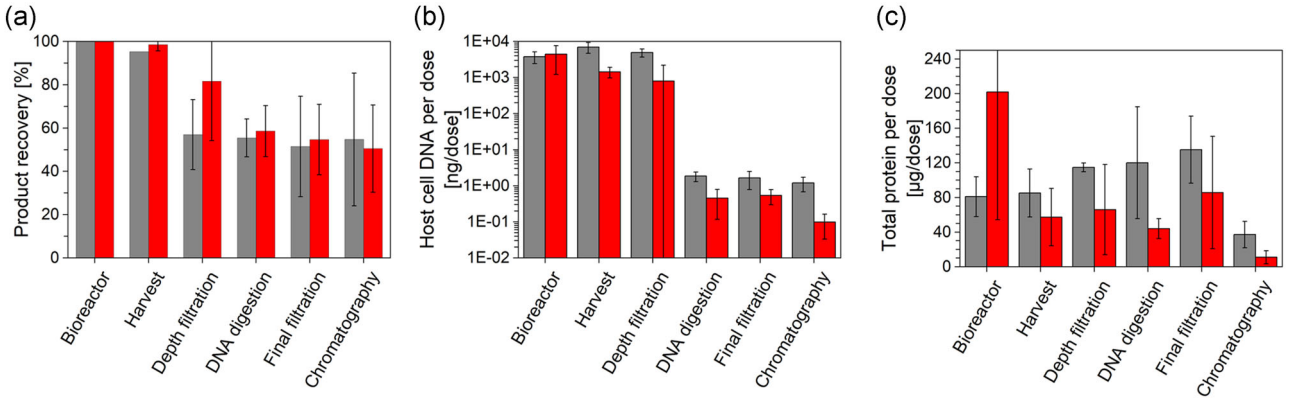

FIGURE 3 Product recovery and impurity removal of the different purification steps for the integrated batch or perfusion processes. (a) Percentage recovery of the total number of infectious virions of individual process steps, (b) level of host cell DNA per dose, and (c) level of total protein per dose of the integrated batch processes (gray) and the integrated perfusion run 1 (red). To estimate contamination levels, a Modified Vaccinia virus Ankara (MVA) dose input of 1.43×10^8 $TCID_{50}$ was assumed (see Section 2.4). The MVA raw material for steric exclusion chromatography was purified in semi-continuous mode, as described in Section 2.3-3. Error bars of the batch process correspond to the standard deviation of triplicate runs, as described in Section 2.4. Error bars of run 1 correspond to the standard deviation of the yields for continuous harvesting between 36 and 87 hpi (time intervals between samples <14 h), as described in Section 2.4

(run 1 only, as perfusion run 2 was not integrated to purification) was equal to 54.7% and 50.5%, respectively (Figure 3a). Recovery for depth filtration was 59.8% and 81.6% for the batch and perfusion processes, respectively. The DNA digestion step allowed for the perfusion and batch process and about 3 $\log_{10}$ depletion of host cell DNA per dose, reaching less than 10 ng host cell DNA/dose (assuming an MVA dose input of 1.43×10^8 $TCID_{50}$; Section 2.4). Compared with the raw material in the bioreactor, the total protein

amount per dose decreased by a factor of 18.3 for the perfusion and 2.2 for the batch process after purification by SXC (final value: 11–37 µg total protein/dose; Figure 3c). When performing a two-sample *t*-test, the decrease of host cell DNA per dose and the decrease of total protein per dose was found to be statistically significant (p value < 0.05) for the perfusion and batch cultivations, respectively. The large error of the host cell protein per dose (perfusion mode) at the bioreactor step (Figure 2a) results from a highly varying virus titer and host cell protein concentration during the continuous virus harvesting. Later on, the variability was decreased for the perfusion process with the use of salts stabilizing the virus and the retention bottles B1–B4. The large error observed for host cell DNA per dose (perfusion mode) after the depth filtration step (Figure 3b) was probably due to partial host cell DNA digestion as endonuclease was added in bottle B2 (Figure 1) and sampling times were different. A STY of 10.5×10^{10} $TCID_{50}/L_{bioreactor}$/day for the perfusion and $1.7 \pm 0.3 \times 10^{10} TCID_{50}/L_{bioreactor}$/day for the batch processes were obtained. This comparison is relevant to assess the impact of the bioreactor footprint on the productivity and the potential of perfusion considering all the aspects from USP to DSP.

3.3 | Control of perfusion rate and evaluation of MVA harvesting time based on online capacitance probe measurements

The perfusion rate during the cell growth phase could be successfully controlled using a capacitance probe for run 1. No offset between the offline VCC and online VCC was observed (Figure 4). A CSPR of 48.0 pL/cell/day was kept constant for at least 3 days before virus infection. The first CSPR value obtained 96 h before infection was estimated too high due to a pump calibration error. No limitation in glucose concentration was observed during the whole run (data not shown). The capacitance probe was not used for run 2 during the cell growth phase.

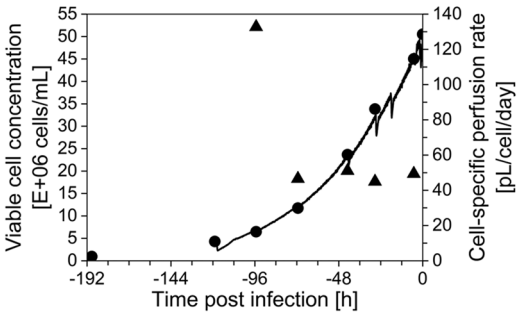

FIGURE 4 Online monitoring of cell concentrations using a capacitance probe for process automation and control during the growth phase of run 1 (AGE1.CR.pIX cells grown in perfusion mode using an acoustic filter). Offline (●) and online (black line) viable cell concentration, cell-specific perfusion rate (▲). The cell factor (described in Section 2.2-2) converting the permittivity signal to a viable cell concentration was equal to 0.57.

During the virus production phase, the trends of the offline VCC followed the same dynamics as for the $\Delta\varepsilon_{max}$ signal (Figures 5a and 5c), except that the values were given every 8–14 h for the offline VCC and every 0.2 h for the online permittivity signal. A correlation between the VCC or the $\Delta\varepsilon_{max}$ signal was observed with the onset of MVA release (defined in Section 2.2-2). For all runs including the batch run, the expected time of MVA release in the supernatant (based on the permittivity signal decrease time point plus 10.6 h; corresponding to the time when about 8%–10% of Vir_{tot} was released from the infected cells) seemed to correlate with the increase of the virus titer in the bioreactor supernatant. At that time point, a titer in the range of $0.5–1.0 \times 10^8$ $TCID_{50}$/ml was reached (Figure 5). By harvesting the perfusion bioreactor 10.6 h after the maximum $\Delta\varepsilon_{max}$ signal or maximum offline VCC was achieved (illustrated by the vertical line in Figure 5), 81%–95% of the produced infectious virions could be harvested (Appendices, Table A2). Note: This time interval (10.6 h) was estimated based on an average value from run 1, run 2, the control run (data from run 4 of Gränicher et al. (2020), performed similarly to runs 1–2) and a batch run (run C) (Table A2, illustrated in Figure 5). For batch run (c), virus release and cell death were delayed (Figure 5c,d). Overall, the maximum permittivity signal was determined between 24 and 48 hpi (Figure 5). We, therefore, suggest that this could help to decide on harvesting time.

3.4 | Economic analysis: Batch versus perfusion

To allow for economic analysis, data for the cost of goods from end-to-end MVA production in batch (average values for runs a–c) were compared to an end-to-end MVA production in perfusion mode. Data from the perfusion cultivations 1 and 2 were used to estimate the average Vir_{tot}, and the process time for the USP part (referred to as "Seed train" and "Cell culture" in Figure 6c). The data from run 1 was used to estimate the costs regarding the DSP part (referred to as "Filtration and DNA digestion" and "Chromatography" in Figure 6c), as only run 1 was integrating USP with DSP.

The capital expenditures (CAPEX), was 10% higher for the perfusion than for the batch process for the 1 L bioreactor scale (Figure 6a). Concerning the operating expenditures (OPEX), the value for the perfusion process was overall 26% higher than for the batch process, which can be attributed to higher labor costs required for the operation of the integrated perfusion process (Figure 6a). More specifically, for both batch and perfusion processes, the highest costs came from the endonuclease used for DNA digestion (30%–32%), followed by costs for cell culture media (21%–25%) and seed virus (13%–27%) (Figure 6b). Costs for filters and SXC membranes were between 5% and 17%. Overall, for the different production steps from the seed train to the SXC, the batch and perfusion processes had a similar cost per dose at the 1 L bioreactor scale, except for the seed train and cell culture step: here, costs for the batch process were about 5.2 and 3.5-fold higher, respectively (Figure 6c). At the 1 L bioreactor scale, the perfusion process allowed to produce about 3.5-fold more doses per year than the batch

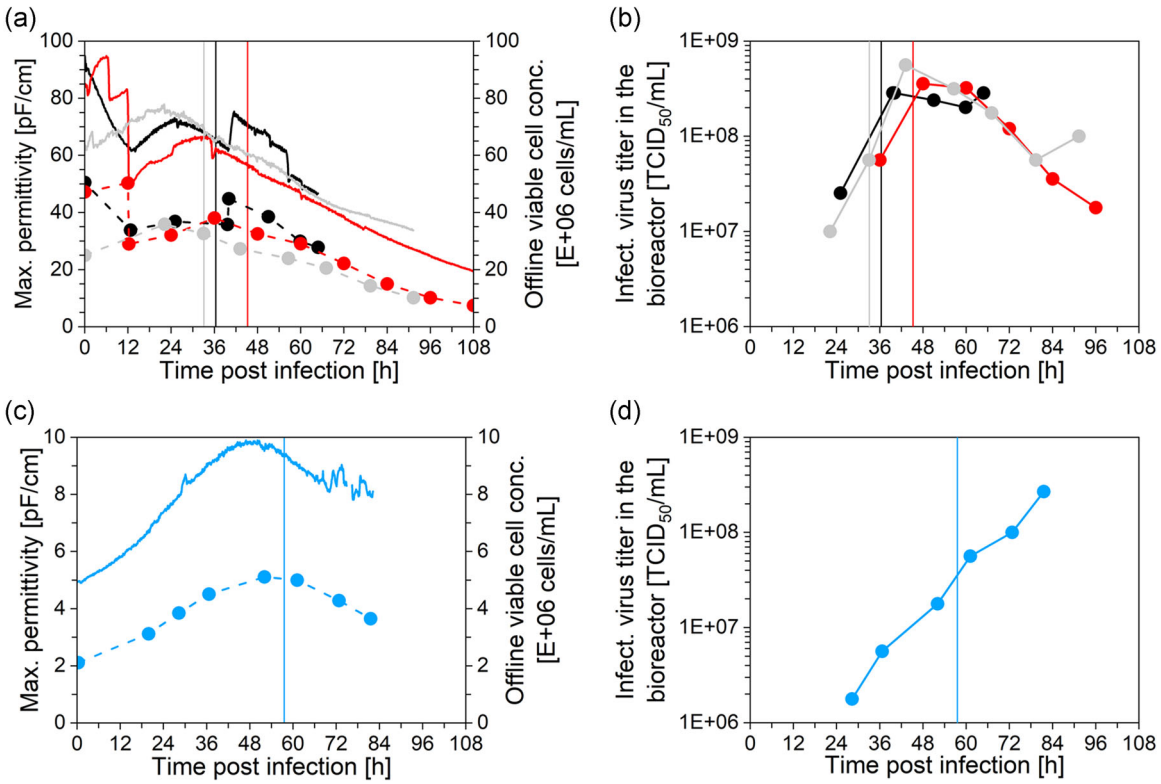

FIGURE 5 Online monitoring of a capacitance probe for process automation and control during Modified Vaccinia virus Ankara (MVA) production using suspension AGE1.CR.pIX cells. (a) Maximum permittivity signal ($\Delta\varepsilon_{max}$; solid line) and offline viable cell concentration (●) for three cultivations in perfusion mode (run 1 = black, run 2 = red, data from run 4 of Gränicher et al. (2020) = gray). (b) Infectious virus titer in the bioreactor supernatant for three cultivations in perfusion mode (run 1 = black, run 2 = red, data from run 4 of Gränicher et al. (2020) = gray). (c) Maximum permittivity signal ($\Delta\varepsilon_{max}$; solid line) and offline viable cell concentration (●) for one cultivation in batch (run c). (d) Infectious virus titer in the bioreactor supernatant for one cultivation in batch mode (run c). The vertical lines (for each run in the respective color) correspond to the expected time of MVA release in the supernatant, which is on average 10.6 h after the maximum permittivity signal (between 12 and 36 h postinfection for perfusion and between 24 and 48 h postinfection for a batch). This time interval of 10.6 h was determined based on the optimal time of virus harvesting for a perfusion process (which is the time of MVA release, corresponding to the time when about 8% to 10% of the total number of infectious virions was released from the infected cells), as described in Section 2.2-2. The cell factor (described in Section 2.2-2) used to convert the permittivity signal to an online viable cell concentration was equal to 0.57, 0.65, and 0.44 for run 1, run 2, and the perfusion control run, respectively

process (Figure 6d). This resulted in a 2.8-fold decrease in cost per dose. At the 1000 L scale, 42 and 147 million doses are projected yearly in the batch and perfusion processes, respectively. Targeting a defined number of doses per year, the perfusion and batch processes showed a similar cost per dose (Figure 6e). Nevertheless, for the same bioreactor scale, the operation of a perfusion system is always advantageous in terms of cost per dose (Figure 6d). At the 200 L scale, the cost per dose for a perfusion process is still 1.8-fold lower than for a batch process. More details about the economic analysis are available in the Appendices.

4 | DISCUSSION

Cell growth, CSVY, and P_v (Figure 2) of the presented perfusion process were in the same range as in previous experiments (Gränicher et al., 2020), with maximum values of 50×10^6 cells/ml, 55.4 $TCID_{50}$/cell, and 2.53×10^{10} $TCID_{50}$/L/day. Still, a rather high variation in P_v was observed for the perfusion runs 1 and 2 (Section 3.1, 1.8-fold P_v decrease for run 2). However, differences in the order of two are commonly found for virus production processes and reflect rather large titration errors and the complexity of the infection cycle (Vazquez-Ramirez et al., 2019). In addition, V_w was increased continuously over a long period for run 1 (2–12 hpi) compared with run 2 (Section 2.2-2). Although no metabolite depletion for run 2 was observed (data not shown), the bolus addition could have decreased the production yield due to not-quantified toxic metabolite accumulation.

The total recovery for the perfusion and batch processes were similar (50.5% and 54.7%, respectively; Figure 4a), showing that the intensified perfusion process did not have a negative impact on cell clarification, host cell DNA removal, and SXC. A total recovery of about 50%–55% is in accordance with results reported from other groups using other DSP processes. Recoveries of 61%–63% for

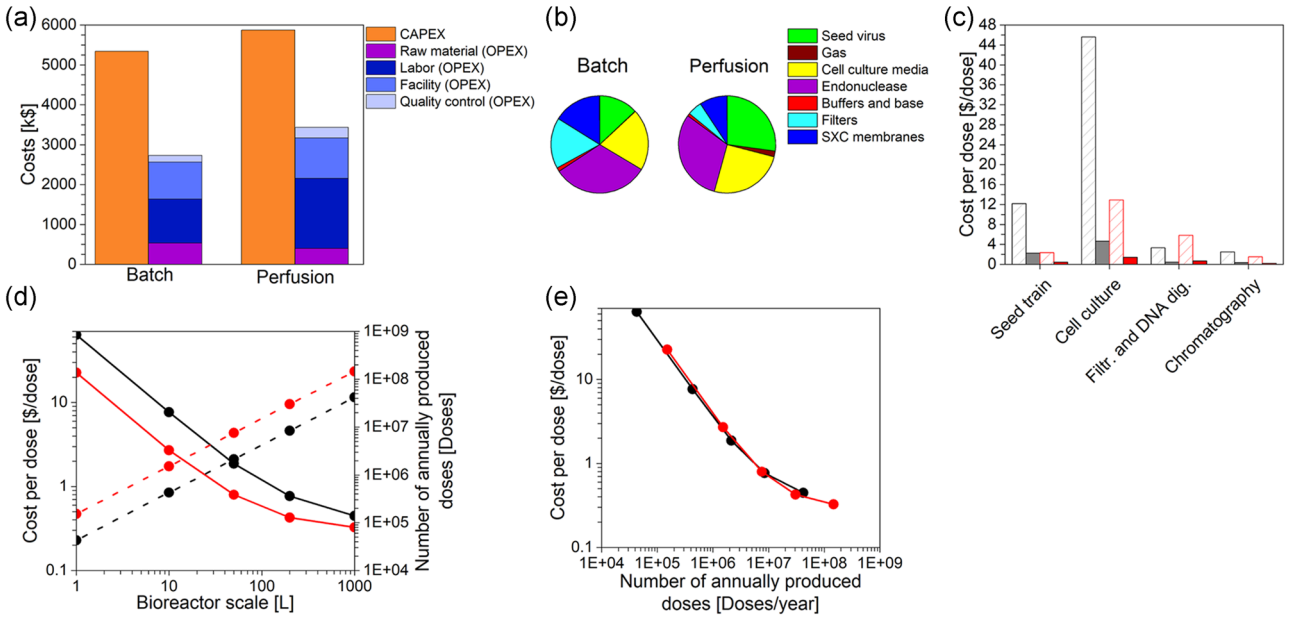

FIGURE 6 Economic analysis for end-to-end production of Modified Vaccinia virus Ankara (MVA) using AGE1.CR.pIX cells cultivated either in batch or in perfusion mode. (a) CAPEX and OPEX of a batch or a perfusion process at the 1 L scale operated over 47 weeks per year. (b) Raw material and consumables costs in batch and perfusion at the 1 L bioreactor scale. (c) Contribution of the seed train, cell culture, filtration plus DNA digestion, and chromatography (SXC) steps on the cost per dose for batch (gray) or perfusion (red), at the 1 L scale (dashed) or at the 10 L scale (full). (d) Cost per dose (solid line) and a number of annually produced doses (dotted line) as a function of the bioreactor scale (1, 10, 50, 200, and 1000 L working volume) for the batch (black) or the perfusion process (red). (e) Cost per dose as a function of the number of annually produced doses. An MVA dose input of 1.43×10^8 $TCID_{50}$ was considered for graphs (c)–(e). For the economic analysis, the SuperPro Designer software was used (Section 2.5). Average data from runs (a)–(c) were used to estimate the costs for an integrated batch process. Average data from runs 1–2 were used to estimate the costs regarding the "Seed train" and the "Cell culture" (c) for the perfusion process. Finally, the data from run 1 were used to estimate the costs of DSP, i.e., "Filtration and DNA digestion" and "Chromatography" (c), as only run 1 was integrating USP with DSP for the perfusion mode

adenovirus (Fernandes et al., 2013; Moleirinho et al., 2020), 41% for MVA (Léon et al. 2016), 52% for influenza virus (Kalbfuss, Wolff, et al., 2007), and 20%–60% for AAV production (Moleirinho et al., 2020; Terova et al., 2018) were reported. Successful application of membrane-based SXC for influenza virus, yellow fever virus, AAV, baculovirus, hepatitis C virus, and Orf virus purifications have been reported (Lothert, Offersgaard, et al., 2020; Lothert, Pagallies, et al., 2020; Lothert, Sprick, et al., 2020; Marichal-Gallardo et al., 2021; Marichal-Gallardo, 2019). This suggests that the integrated process established here may also be transferrable to other virus manufacturing processes (Bissinger et al., 2021). The short purification cycles of the SXC method (of about 40 min) allowed simplifying the semi-continuous purification process. In addition, the less complex bind-elute steps in single-column SXC require fewer optimizations than conventional multi-column chromatography trains (Gerstweiler et al., 2021; Patil & Walther, 2018).

Clarification steps are particularly challenging due to the large size of MVA particles (250–350 nm) and cell lysis at late infection stages. Here, a depth filtration recovery of 59.8%–81.6% (Figure 2) was observed for batch and perfusion cultivations, and depth filtration was the main cause for the reduction of process yields. Similar findings were reported for large-scale manufacturing of vaccinia viruses with depth filters with less than 5 µm pore size (Léon et al. 2016; Ungerechts et al., 2016). Other publications reported recoveries of 85%–90% when using polypropylene depth filters with pore sizes of 0.45–0.60 µm after a centrifugation step, or from the supernatant of an adherent cell culture for smaller viruses such as adenovirus (Fernandes et al., 2013), hepatitis C virus-like particles (Xenopoulos, 2015) or influenza virus (Kalbfuss, Genzel, et al., 2007). Recoveries up to 74% for clarification of vaccinia virus raw material (centrifuged cell lysate and 1:5 diluted in 0.5 M ammonium sulfate and 3 M NaCl) with 0.8 µm cellulose acetate filter were also reported (Vincent, 2017). The polypropylene material used here for depth filtration seems well suited for clarification of virus-containing supernatants and is relatively inert (Besnard et al., 2016; Cherradi et al., 2018) with a surface tension energy lower than other common materials such as polyethylene, polyethylene sulfone or polystyrene membranes (Fenouillot et al., 2009; Kim et al., 2010). In addition, this material largely prevents electrostatic interaction with virus particles (MVA carries a high negative charge at neutral pH (Michen & Graule, 2010)) in contrast to diatomaceous earth, which is a standard material used for depth filtration (lower recovery observed and data not shown) (Besnard et al., 2016; Cherradi et al., 2018). In addition, the adjustment of appropriate salt concentrations also improved yields in-depth filtration (Section 2.3-1, data not shown). This corresponds to previous findings that demonstrated that salt addition reduced the

interaction of virus particles with cell debris and DNA (Hughes et al., 2007; Jordan et al., 2015) and suppressed the aggregation of viral vectors (Wright et al., 2005).

Host cell DNA is one of the most critical and persistent contamination in virus particle purification. Inline endonuclease treatment efficiently reduced host cell DNA levels before subsequent SXC purification. The use of chaotropes for efficient DNA digestion was also essential, as it helped to separate DNA from the surface of viral particles (Jordan et al., 2015). A host cell DNA reduction of around 500-fold was needed for the perfusion process established here (-Figure 3b) to meet the requirements typically set by regulatory authorities (<10 ng/dose). The establishment of this novel continuous inline DNA digestion step was inspired by the use of plug flow reactors with immobilized enzymes (Pitcher, 1978), and resulted in an over 10,000-fold reduction of DNA (Figure 3b). Unlike chemostats, plug flow reactors allow a narrow distribution of the residence time.

The perfusion rate was controlled via estimation of the VCC by an online capacitance probe (Figure 4). Similar findings were reported by Nikolay et al. (2018) for a different avian cell line. It thus seems that this technique is a versatile method (Nikolay et al., 2020; Wu et al., 2021) as long as the diameter of the cells remains constant during the time course of cultivations. There are several options to correlate the permittivity signal with the VCC (Cannizzaro et al., 2003). For our case, a simple linear regression between the permittivity signal and the offline VCC was precise enough to determine the VCC during the cell growth phase. During the virus production process, the time of MVA release (term defined in Section 2.2-2) could be determined with $\Delta\varepsilon_{max}$ or offline VCC with a precision of about ± 4 h, over four different runs in perfusion or batch mode (Figure 5). To determine the time of MVA release, the use of $\Delta\varepsilon_{max}$ online monitoring is more useful than offline VCC measurements since the analysis is more frequent. Previous publications already reported the use of the permittivity signal to estimate the optimum time of harvest for measles virus (Grein et al., 2018) and adeno-associated vector production (Negrete et al., 2007). Petiot et al. (2017) used $\Delta\varepsilon_{max}$ and critical frequency (Fc) values to determine changes in C_m and σ_i values to monitor the progress of infection for different enveloped (e.g., lentivirus, influenza virus) and nonenveloped (reovirus) viruses. In our case, monitoring of Fc, C_m, and σ_i did not lead to unambiguous results (Appendices). More cultivations should be performed to infer a correlation between the permittivity signal and MVA release for process monitoring (Figure 5 and Appendices, Table A2). This is in particular important for perfusion processes, were the time point of significant virus release needs to be identified for initiation of subsequent process steps, that is, chromatographic purification. Furthermore, it would support the establishment of robust processes following the guidelines of the PAT initiative (FDA, 2004).

To assess the benefit of integrated perfusion processes, an economic analysis was performed using SuperPro designer software. Based on the results shown in Figure 6, the cost per MVA dose could be reduced by a factor of 2.8 for production in perfusion mode at the 1 L scale (compared with the batch processes). This is due to the higher virus production yield in USP (also shown earlier by Gränicher et al., 2020), while achieving a similar overall recovery in the purification train (Sections 3.1–3.2). The use of a perfusion system allowed to increase virus production while keeping the same bioreactor footprint (STY > 6 times higher for virus production in perfusion mode compared to batch mode). Although operation of the perfusion system is more labor-intensive, the cost per dose was lower as the production capacity increased by a factor of 3.5 (1 L scale). Furthermore, the seed train costs were decreased as fewer bioreactor runs per year need to be performed (53 runs in batch mode vs. 31 runs in perfusion mode, see Appendices) and a higher STY was observed for the perfusion process (Figure 6). Costs were mainly reduced for the seed train and USP when intensifying and scaling up the production process (Figure 6c), similarly to what was observed for AAV (Cameau et al., 2019) and lentivirus manufacturing (Comisel et al., 2020). Higher costs for seed virus for perfusion over batch processes were estimated (Figure 6b), as cultures are infected at a higher VCC and, to keep the MOI, more virus is needed (>10-fold; Section 2.2). Nevertheless, process time was not drastically prolonged (Appendices). The cell culture media cost was not higher for the perfusion process (Figure 6b) because the CSPR was kept to a minimum and, although the perfusion cultivations need higher media volumes, more viruses can be produced than in batch. As also observed in AAV manufacturing, the establishment of intensified USP systems has little impact on the DSP cost per dose (Cameau et al., 2019), although the chromatography method used was different for both cases. Concerning raw materials and consumables costs, the significant costs for DNA digestion could be further reduced by optimizing the endonuclease treatment step in the future. Finally, the low costs of the SXC purification step led to a very low contribution to the overall consumable stocks, in contrast to other DSP techniques that required expensive resins or coated surfaces (Comisel et al., 2020).

So far, few studies have addressed bioprocess economics for the production of viral vectors (Cameau et al., 2019; Comisel et al., 2020) or virus-like particles (Chuan et al., 2014). For all of them, using suspension cell culture in batch mode appeared to be the most cost-effective option. Here, suspension cell culture in perfusion mode is presented as an additional option to further reduce costs. Although for a fixed amount of MVA doses per year the perfusion process would not decrease the cost per dose compared with a batch process, the CAPEX is not the same across scales for batch and perfusion systems. For example, a 200 L batch bioreactor is predicted to produce as much as a 50 L perfusion bioreactor ($7.6–8.4 \times 10^6$ doses per year). Although the cost per dose is not reduced for the perfusion system, the CAPEX is about 1.2-fold lower resulting in a faster return of investments (Appendices). In addition, the use of perfusion systems is always advantageous for the same bioreactor scale (Figure 6), which might be of interest for modification of existing virus manufacturing plants towards an increase of product output.

As an outlook, the recovery of the integrated process could be further increased by optimizing the first depth filtration step, as this resulted in the most significant drop in virus titers (Figure 3a). For instance, depth filters with larger pore sizes could be added before

the used depth filter, to remove more efficiently large cell debris without product retention. The concentration of the salt used as a chaotropic agent could also be re-evaluated. Indeed, an increase in the ionic strength might decrease the zeta potential of the membrane below a critical value. As a result, the electrostatic repulsion between the feed and the membrane could be decreased resulting in membrane fouling, unspecific product adsorption or aggregation of flocs that may also contain virus particles (Breite et al., 2016; Lukasik et al., 2000).

In conclusion, an integrated perfusion process for MVA production has been established with a minimum of clarification and purification steps. An overall product recovery of 50.5% was achieved, allowing to increase the STY by 600% compared with a batch system operated at the same scale. This was mainly due to the fact, that the virus production phase could be kept constant for both processes. Furthermore, the observed purification performance of membrane-based SXC was not hampered due to cell culture process intensification. The use of an online capacitance probe allowed the control of the perfusion rate during the cell growth phase and indicated the time of MVA release to initiate subsequent processing steps. Finally, a detailed cost analysis, based on several runs performed in batch and perfusion mode, indicated that the cost per dose in MVA production would be decreased by a factor of 2.8 if the system would be operated in perfusion mode at the 1 L scale.

ACKNOWLEDGMENTS

The authors would like to thank Anja Bastian, Claudia Best, Ilona Behrendt, and Nancy Wynserski for their excellent technical support and Andrea Schneider (Sartorius AG) for providing depth filters for material screening. This study was financed by the Max Planck Society. Open Access funding enabled and organized by Projekt DEAL.

CONFLICT OF INTERESTS

Gwendal Gränicher, Masoud Babakhani, Sven Göbel, and Yvonne Genzel declare that they have no conflict of interest. Pavel Marichal-Gallardo and Udo Reichl are inventors of a pending patent application describing the SXC virus purification technology used in this study. Ingo Jordan is an employee of ProBioGen AG, which has established the AGE1.CR.pIX cell line, the MVA-CR19.GFP and the CD-U5 medium.

ETHICAL APPROVAL

This article does not contain any studies with human participants or animals performed by any of the authors.

AUTHOR CONTRIBUTIONS

Gwendal Gränicher, Pavel Marichal-Gallardo, Ingo Jordan, Yvonne Genzel, and Udo Reichl contributed to the conception and design of the study. Gwendal Gränicher, Sven Göbel, and Masoud Babakhani performed the experiments and process modeling. Gwendal Gränicher and Masoud Babakhani analyzed the data. Gwendal Gränicher wrote the manuscript. All authors contributed to manuscript revision, read, and approved the submitted version.

DATA AVAILABILITY STATEMENT

Data available in article supplementary material. Additional data is available on request from the authors. The data that support the findings of this study are available from the corresponding author, Yvonne Genzel, upon reasonable request.

ORCID

Gwendal Gränicher http://orcid.org/0000-0002-6572-841X

REFERENCES

Allison, G., Cain, Y. T., Cooney, C., Garcia, T., Bizjak, T. G., Holte, O., Jagota, N., Komas, B., Korakianiti, E., Kourti, D., Madurawe, R., Morefield, E., Montgomery, F., Nasr, M., Randolph, W., Robert, J. L., Rudd, D., & Zezza, D. (2015). Regulatory and quality considerations for continuous manufacturing may 20–21, 2014 continuous manufacturing symposium. *Journal of Pharmaceutical Sciences*, *104*(3), 803–812. https://doi.org/10.1002/jps.24324

ATCC. (2012). FAQ's: Converting TCID[50] to plaque forming units (PFU): Is it possible to determine from the TCID[50] how many plaque forming units to expect?

Besnard, L., Fabre, V., Fettig, M., Gousseinov, E., Kawakami, Y., Laroudie, N., Scanlan, C., & Pattnaik, P. (2016). Clarification of vaccines: An overview of filter based technology trends and best practices. *Biotechnology Advances*, *34*(1), 1–13. https://doi.org/10.1016/j.biotechadv.2015.11.005

Bielser, J. M., Wolf, M., Souquet, J., Broly, H., & Morbidelli, M. (2018). Perfusion mammalian cell culture for recombinant protein manufacturing - A critical review. *Biotechnology Advances*, *36*(4), 1328–1340. https://doi.org/10.1016/j.biotechadv.2018.04.011

Bissinger, T., Wu, Y., Marichal-Gallardo, P., Riedel, D., Liu, X., Genzel, Y., Tan, W, & Reichl, U. (2021). Integrated production of an influenza A vaccine candidate with MDCK suspension cells. *Authorea*. https://doi.org/10.22541/au.161476429.90376721/v1

Breite, D., Went, M., Prager, A., & Schulze, A. (2016). The critical zeta potential of polymer membranes: How electrolytes impact membrane fouling. *RSC Advances*, *6*(100), 98180–98189. https://doi.org/10.1039/C6RA19239D

Cameau, E., Pedregal, A., & Glover, C. (2019). Cost modelling comparison of adherent multi-trays with suspension and fixed-bed bioreactors for the manufacturing of gene therapy products. *Cell and Gene Therapy Insights*, *5*(11), 1663–1674. https://doi.org/10.18609/cgti.2019.175

Cannizzaro, C., Gügerli, R., Marison, I., & von Stockar, U. (2003). On-line biomass monitoring of CHO perfusion culture with scanning dielectric spectroscopy. *Biotechnology and Bioengineering*, *84*(5), 597–610. https://doi.org/10.1002/bit.10809

Cherradi, Y., Le Merdy, S., Sim, L.-J., Ito, T., Pattanaik, P., Haas, J., & Boumlic, A. (2018). Filter-based clarification of viral vaccines and vectors. *BioProcess International*, *16*(4), 48–53.

Chuan, Y. P., Wibowo, N., Lua, L. H. L., & Middelberg, A. P. J. (2014). The economics of virus-like particle and capsomere vaccines. *Biochemical Engineering Journal*, *90*, 255–263. https://doi.org/10.1016/j.bej.2014.06.005

Comisel, R. -M., Kara, B., Fiesser, F. H., & Farid, S. S. (2020). Lentiviral vector bioprocess economics for cell and gene therapy commercialisation. *Biochemical Engineering Journal*, *167*, 107868. https://doi.org/10.1016/j.bej.2020.107868

FDA. (2004). Guidance for industry PAT: A framework for innovative pharmaceutical development, manufacturing and quality assurance: Rockville.

Fenouillot, F., Cassagnau, P., & Majesté, J. C. (2009). Uneven distribution of nanoparticles in immiscible fluids: Morphology development in polymer blends. *Polymer*, *50*(6), 1333–1350. https://doi.org/10.1016/j.polymer.2008.12.029

Fernandes, P., Peixoto, C., Santiago, V. M., Kremer, E. J., Coroadinha, A. S., & Alves, P. M. (2013). Bioprocess development for canine adenovirus type 2 vectors. *Gene Therapy*, *20*(4), 353–360. https://doi.org/10.1038/gt.2012.52

Genzel, Y., Vogel, T., Buck, J., Behrendt, I., Ramirez, D. V., Schiedner, G., Jordan, I., & Reichl, U. (2014). High cell density cultivations by alternating tangential flow (ATF) perfusion for influenza A virus production using suspension cells. *Vaccine*, *32*(24), 2770–2781. https://doi.org/10.1016/j.vaccine.2014.02.016

Gerstweiler, L., Bi, J., & Middelberg, A. P. J. (2021). Continuous downstream bioprocessing for intensified manufacture of biopharmaceuticals and antibodies. *Chemical Engineering Science*, *231*, 116272. https://doi.org/10.1016/j.ces.2020.116272

Godawat, R., Konstantinov, K., Rohani, M., & Warikoo, V. (2015). End-to-end integrated fully continuous production of recombinant monoclonal antibodies. *Journal of Biotechnology*, *213*, 13–19. https://doi.org/10.1016/j.jbiotec.2015.06.393

Gränicher, G., Coronel, J., Trampler, F., Jordan, I., Genzel, Y., & Reichl, U. (2020). Performance of an acoustic settler versus a hollow fiber-based ATF technology for influenza virus production in perfusion. *Applied Microbiology and Biotechnology*, *104*, 4877–4888. https://doi.org/10.1007/s00253-020-10596-x

Gränicher, G., Tapia, F., Behrendt, I., Jordan, I., Genzel, Y., & Reichl, U. (2020). Production of Modified Vaccinia Ankara Virus by intensified cell cultures: A comparison of platform technologies for viral vector production. *Biotechnology Journal*, *16*, 2000024. https://doi.org/10.1002/biot.202000024

Grein, T. A., Loewe, D., Dieken, H., Salzig, D., Weidner, T., & Czermak, P. (2018). High titer oncolytic measles virus production process by integration of dielectric spectroscopy as online monitoring system. *Biotechnology and Bioengineering*, *115*(5), 1186–1194. https://doi.org/10.1002/bit.26538

Hughes, K., Zachertowska, A., Wan, S., Li, L., Klimaszewski, D., Euloth, M., & Hatchette, T. F. (2007). Yield increases in intact influenza vaccine virus from chicken allantoic fluid through isolation from insoluble allantoic debris. *Vaccine*, *25*(22), 4456–4463. https://doi.org/10.1016/j.vaccine.2007.03.017

Jordan, I., Horn, D., Thiele, K., Haag, L., Fiddeke, K., & Sandig, V. (2020). A deleted deletion site in a new vector strain and exceptional genomic stability of plaque-purified Modified Vaccinia Ankara (MVA). *Virologica Sinica*, *35*(1), 212–226. https://doi.org/10.1007/s12250-019-00176-3

Jordan, I., Northoff, S., Thiele, M., Hartmann, S., Horn, D., Höwing, K., Bernhardt, H., Oehmke, S., von Horsten, H., Rebeski, D., Hinrichsen, L., Zelnik, V., Mueller, W., & Sandig, V. (2011). A chemically defined production process for highly attenuated poxviruses. *Biologicals*, *39*(1), 50–58. https://doi.org/10.1016/j.biologicals.2010.11.005

Jordan, I., Weimer, D., Iarusso, S., Bernhardt, H., Lohr, V., & Sandig, V. (2015). Purification of modified vaccinia virus Ankara from suspension cell culture. *BMC Proceedings*, *9*(suppl 9):O13. https://doi.org/10.1186/1753-6561-9-S9-O13

Justice, C., Brix, A., Freimark, D., Kraume, M., Pfromm, P., Eichenmueller, B., & Czermak, P. (2011). Process control in cell culture technology using dielectric spectroscopy. *Biotechnology Advances*, *29*(4), 391–401. https://doi.org/10.1016/j.biotechadv.2011.03.002

Kaemmerer, W. F. (2018). How will the field of gene therapy survive its success? *Bioengineering & Translational Medicine*, *3*(2), 166–177. https://doi.org/10.1002/btm2.10090

Kalbfuss, B., Genzel, Y., Wolff, M., Zimmermann, A., Morenweiser, R., & Reichl, U. (2007). Harvesting and concentration of human influenza A virus produced in serum-free mammalian cell culture for the production of vaccines. *Biotechnology and Bioengineering*, *97*(1), 73–85. https://doi.org/10.1002/bit.21139

Kalbfuss, B., Wolff, M., Morenweiser, R., & Reichl, U. (2007). Purification of cell culture-derived human influenza A virus by size-exclusion and anion-exchange chromatography. *Biotechnology and Bioengineering*, *96*(5), 932–944. https://doi.org/10.1002/bit.21109

Karst, D. J., Steinebach, F., & Morbidelli, M. (2018). Continuous integrated manufacturing of therapeutic proteins. *Current Opinion in Biotechnology*, *53*, 76–84. https://doi.org/10.1016/j.copbio.2017.12.015

Karst, D. J., Steinebach, F., Soos, M., & Morbidelli, M. (2017). Process performance and product quality in an integrated continuous antibody production process. *Biotechnology and Bioengineering*, *114*(2), 298–307. https://doi.org/10.1002/bit.26069

Kim, Y., Rana, D., Matsuura, T., Chung, W. -J., & Khulbe, K. C. (2010). Relationship between surface structure and separation performance of poly(ether sulfone) ultra-filtration membranes blended with surface modifying macromolecules. *Separation and Purification Technology*, *72*(2), 123–132. https://doi.org/10.1016/j.seppur.2010.01.006

Klutz, S., Holtmann, L., Lobedann, M., & Schembecker, G. (2016). Cost evaluation of antibody production processes in different operation modes. *Chemical Engineering Science*, *141*, 63–74. https://doi.org/10.1016/j.ces.2015.10.029

Konstantinov, K. B., & Cooney, C. L. (2015). White paper on continuous bioprocessing May 20–21 2014 continuous manufacturing symposium. *Journal of Pharmaceutical Sciences*, *104*(3), 813–820. https://doi.org/10.1002/jps.24268

Léon, A., David, A. L., Madeline, B., Guianvarc'h, L., Dureau, E., Champion-Arnaud, P., Hebben, M., Huss, T., Chatrenet, B., & Schwamborn, K. (2016). The EB66(R) cell line as a valuable cell substrate for MVA-based vaccines production. *Vaccine*, *34*(48), 5878–5885. https://doi.org/10.1016/j.vaccine.2016.10.043

Lim, A. C., Washbrook, J., Titchener-Hooker, N. J., & Farid, S. S. (2006). A computer-aided approach to compare the production economics of fed-batch and perfusion culture under uncertainty. *Biotechnology and Bioengineering*, *93*(4), 687–697. https://doi.org/10.1002/bit.20757

Lohr, V. (2014). *Characterization of the avian designer cells AGE1.CR and AGE1.CR.pIX considering growth, metabolism and production of influenza virus and Modified Vaccinia Virus Ankara (MVA)* (dissertation, PhD Thesis). Magdeburg: Otto-von-Guericke Universität. http://hdl.handle.net/11858/00-001M-0000-0024-3EDE-2

Lothert, K., Offersgaard, A. F., Pihl, A. F., Mathiesen, C. K., Jensen, T. B., Alzua, G. P., Fahnøe, U., Bukh, J., Gottwein, J. M., & Wolff, M. W. (2020). Development of a downstream process for the production of an inactivated whole hepatitis C virus vaccine. *Scientific Reports*, *10*(1), 16261. https://doi.org/10.1038/s41598-020-72328-5

Lothert, K., Pagallies, F., Feger, T., Amann, R., & Wolff, M. W. (2020). Selection of chromatographic methods for the purification of cell culture-derived Orf virus for its application as a vaccine or viral vector. *Journal of Biotechnology*, *323*, 62–72. https://doi.org/10.1016/j.jbiotec.2020.07.023

Lothert, K., Sprick, G., Beyer, F., Lauria, G., Czermak, P., & Wolff, M. W. (2020). Membrane-based steric exclusion chromatography for the purification of a recombinant baculovirus and its application for cell therapy. *Journal of Virological Methods*, *275*, 113756. https://doi.org/10.1016/j.jviromet.2019.113756

Lukasik, J., Scott, T. M., Andryshak, D., & Farrah, S. R. (2000). Influence of salts on virus adsorption to microporous filters. *Applied and Environmental Microbiology*, *66*(7), 2914–2920. https://doi.org/10.1128/aem.66.7.2914-2920.2000

Manceur, A. P., Kim, H., Misic, V., Andreev, N., Dorion-Thibaudeau, J., Lanthier, S., Bernier, A., Tremblay, S., Gélinas, A. M., Broussau, S., Gilbert, R., & Ansorge, S. (2017). Scalable lentiviral vector production using stable HEK293SF producer cell lines. *Human Gene Therapy Methods*, *28*(6), 330–339. https://doi.org/10.1089/hgtb.2017.086

Marichal-Gallardo, P. (2019). *Chromatographic purification of biological macromolecules by their capture on hydrophilic surfaces with the aid of non-ionic polymers* (PhD Thesis). Magdeburg: Otto-von-Guericke-Universität. https://pure.mpg.de/rest/items/item_3248240/component/file_3249620/content

Marichal-Gallardo, P., Börner, K., Pieler, M. M., Sonntag-Buck, V., Obr, M., Bejarano, D., Wolff, M. W., Kräusslich, H. G., Reichl, U., & Grimm, D. (2021). Single-use capture purification of adeno-associated viral gene transfer vectors by membrane-based steric exclusion chromatography. *Human Gene Therapy*. https://doi.org/10.1089/hum.2019.284

Marichal-Gallardo, P., Pieler, M. M., Wolff, M. W., & Reichl, U. (2017). Steric exclusion chromatography for purification of cell culture-derived influenza A virus using regenerated cellulose membranes and polyethylene glycol. *Journal of Chromatography A*, *1483*, 110–119. https://doi.org/10.1016/j.chroma.2016.12.076

Michen, B., & Graule, T. (2010). Isoelectric points of viruses. *Journal of Applied Microbiology*, *109*(2), 388–397. https://doi.org/10.1111/j.1365-2672.2010.04663.x

Moleirinho, M. G., Silva, R. J. S., Alves, P. M., Carrondo, M. J. T., & Peixoto, C. (2020). Current challenges in biotherapeutic particles manufacturing. *Expert Opinion on Biological Therapy*, *20*(5), 451–465. https://doi.org/10.1080/14712598.2020.1693541

Negrete, A., Esteban, G., & Kotin, R. M. (2007). Process optimization of large-scale production of recombinant adeno-associated vectors using dielectric spectroscopy. *Applied Microbiology and Biotechnology*, *76*(4), 761–772. https://doi.org/10.1007/s00253-007-1030-9

Nikolay, A., Bissinger, T., Gränicher, G., Wu, Y., Genzel, Y., & Reichl, U. (2020). Perfusion control for high cell density cultivation and viral vaccine production. In R. Pörtner (Ed.), *Animal cell biotechnology* (Vol. 2095, pp. 141–168). Humana Press.

Nikolay, A., Leon, A., Schwamborn, K., Genzel, Y., & Reichl, U. (2018). Process intensification of EB66(R) cell cultivations leads to high-yield yellow fever and Zika virus production. *Applied Microbiology and Biotechnology*, *102*(1), 8725–8737. https://doi.org/10.1007/s00253-018-9275-z

Patil, R., & Walther, J. (2018). Continuous manufacturing of recombinant therapeutic proteins: Upstream and downstream technologies. In B. Kiss, U. Gottschalk, & M. Pohlscheidt (Eds.), *New bioprocessing strategies: Development and manufacturing of recombinant antibodies and proteins* (pp. 277–322). Springer International Publishing.

Pearson, S. (2020). Process intensification of viral-based vaccines. Where are the bottlenecks? *BioProcess International*, *18*(6), 68–70.

Petiot, E., Ansorge, S., Rosa-Calatrava, M., & Kamen, A. (2017). Critical phases of viral production processes monitored by capacitance. *Journal of Biotechnology*, *242*, 19–29. https://doi.org/10.1016/j.jbiotec.2016.11.010

Petiot, E., Jacob, D., Lanthier, S., Lohr, V., Ansorge, S., & Kamen, A. A. (2011). Metabolic and Kinetic analyses of influenza production in perfusion HEK293 cell culture. *BMC Biotechnology*, *11*(84), 1–12. https://doi.org/10.1186/1472-6750-11-84

Pinto, N. D. S., Napoli, W. N., & Brower, M. (2019). Impact of micro and macroporous TFF membranes on product sieving and chromatography loading for perfusion cell culture. *Biotechnology and Bioengineering*, *117*, 117–124. https://doi.org/10.1002/bit.27192

Pitcher, W. H. (1978). *Design and operation of immobilized enzyme reactors*. Springer.

Pleitt, K., Somasundaram, B., Johnson, B., Shave, E., & Lua, L. H. L. (2019). Evaluation of process simulation as a decisional tool for biopharmaceutical contract development and manufacturing organizations. *Biochemical Engineering Journal*, *150*, 107252. https://doi.org/10.1016/j.bej.2019.107252

Pollock, J., Ho, S. V., & Farid, S. S. (2013). Fed-batch and perfusion culture processes: Economic, environmental, and operational feasibility under uncertainty. *Biotechnology and Bioengineering*, *110*(1), 206–219. https://doi.org/10.1002/bit.24608

Tapia, F., Vazquez-Ramirez, D., Genzel, Y., & Reichl, U. (2016). Bioreactors for high cell density and continuous multi-stage cultivations: options for process intensification in cell culture-based viral vaccine production. *Applied Microbiology and Biotechnology*, *100*(5), 2121–2132. https://doi.org/10.1007/s00253-015-7267-9

Terova, O., Soltys, S., Hermans, P., De Rooij, J., & Detmers, F. (2018). Overcoming downstream purification challenges for viral vector manufacturing: enabling advancement of gene therapies in the clinic. *Cell & Gene Therapy Insights*, *4*(2), 101–111. https://doi.org/10.18609/CGTI.2018.017

Ungerechts, G., Bossow, S., Leuchs, B., Holm, P. S., Rommelaere, J., Coffey, M., Coffin, R., Bell, J., & Nettelbeck, D. M. (2016). Moving oncolytic viruses into the clinic: Clinical-grade production, purification, and characterization of diverse oncolytic viruses. *Molecular Therapy - Methods & Clinical Development*, *3*, 16018. https://doi.org/10.1038/mtm.2016.18

Van der Loo, J. C. M., & Wright, J. F. (2015). Progress and challenges in viral vector manufacturing. *Human Molecular Genetics*, *25*(R1), R42–R52. https://doi.org/10.1093/hmg/ddv451

Vazquez-Ramirez, D., Jordan, I., Sandig, V., Genzel, Y., & Reichl, U. (2019). High titer MVA and influenza A virus production using a hybrid fed-batch/perfusion strategy with an ATF system. *Applied Microbiology and Biotechnology*, *103*(1), 3025–3035. https://doi.org/10.1007/s00253-019-09694-2

Vincent, D. I. W. (2017). *Purification of recombinant vaccinia virus for oncolytic and immunotherapeutic applications using monolithic column technology*. University College London. https://discovery.ucl.ac.uk/id/eprint/10038211

Walther, J., Godawat, R., Hwang, C., Abe, Y., Sinclair, A., & Konstantinov, K. (2015). The business impact of an integrated continuous biomanufacturing platform for recombinant protein production. *Journal of Biotechnology*, *213*(1), 3–12. https://doi.org/10.1016/j.jbiotec.2015.05.010

Walther, J., Lu, J., Hollenbach, M., Yu, M., Hwang, C., McLarty, J., & Brower, K. (2019). Perfusion cell culture decreases process and product heterogeneity in a head-to-head comparison with fed-batch. *Biotechnology Journal*, *14*(2), 1–10. https://doi.org/10.1002/biot.201700733

Wang, S., Godfrey, S., Ravikrishnan, J., Lin, H., Vogel, J., & Coffman, J. (2017). Shear contributions to cell culture performance and product recovery in ATF and TFF perfusion systems. *Journal of Biotechnology*, *246*, 52–60. https://doi.org/10.1016/j.jbiotec.2017.01.020

Wang, S. B., Godfrey, S., Radoniqi, F., Lin, H., & Coffman, J. (2019). Larger pore size hollow fiber membranes as a solution to the product retention issue in filtration-based perfusion bioreactors. *Biotechnology Journal*, *14*(2), 1800137. https://doi.org/10.1002/biot.201800137

Warikoo, V., Godawat, R., Brower, K., Jain, S., Cummings, D., Simons, E., Johnson, T., Walther, J., Yu, M., Wright, B., McLarty, J., Karey, K. P., Hwang, C., Zhou, W., Riske, F., & Konstantinov, K. (2012). Integrated continuous production of recombinant therapeutic proteins.

Biotechnology and Bioengineering, *109*(12), 3018–3029. https://doi.org/10.1002/bit.24584

Wright, J. F., Le, T., Prado, J., Bahr-Davidson, J., Smith, P. H., Zhen, Z., Sommer, J. M., Pierce, G. F., & Qu, G. (2005). Identification of factors that contribute to recombinant AAV2 particle aggregation and methods to prevent its occurrence during vector purification and formulation. *Molecular Therapy*, *12*(1), 171–178. https://doi.org/10.1016/j.ymthe.2005.02.021

Wu, Y., Bissinger, T., Genzel, Y., Liu, X., Reichl, U., & Tan, W.-S. (2021). High cell density perfusion process for high yield of influenza A virus production using MDCK suspension cells. *Applied Microbiology and Biotechnology*, *105*(4), 1421–1434. https://doi.org/10.1007/s00253-020-11050-8

Wyatt, L. S., Earl, P. L., Eller, L. A., & Moss, B. (2004). Highly attenuated smallpox vaccine protects mice with and without immune deficiencies against pathogenic vaccinia virus challenge. *Proceedings of the National Academy of Sciences of the United States of America*, *101*(13), 4590–4595. https://doi.org/10.1073/pnas.0401165101

Xenopoulos, A. (2015). *Production and purification of hepatitis C virus-like particles* [Webinar]. EMD Millipore Webinar Series.

Xu, S., & Chen, H. (2016). High-density mammalian cell cultures in stirred-tank bioreactor without external pH control. *Journal of Biotechnology*, *231*, 149–159. https://doi.org/10.1016/j.jbiotec.2016.06.019

SUPPORTING INFORMATION

Additional supporting information may be found in the online version of the article at the publisher's website.

How to cite this article: Gränicher, G., Babakhani, M., Göbel, S., Jordan, I., Marichal-Gallardo, P., Genzel, Y., & Reichl, U. (2021). A high cell density perfusion process for Modified Vaccinia virus Ankara production: Process integration with inline DNA digestion and cost analysis. *Biotechnology and Bioengineering*, 118, 4720–4734. https://doi.org/10.1002/bit.27937